Aging, Yielding, and Shear Banding in Soft Colloidal Glasses

S. A. Rogers,[1] D. Vlassopoulos,[2] and P. T. Callaghan[1,*]

[1]*MacDiarmid Institute for Advanced Materials and Nanotechnologies, Victoria University of Wellington, Wellington, New Zealand*

[2]*FORTH, Institute of Electronic Structure and Laser, Department of Materials Science and Technology, University of Crete,
GR-71110 Heraklion, Crete, Greece*

(Received 1 November 2007; published 28 March 2008)

Soft colloidal interactions in colloidal glasses are modeled using suspensions of multiarm star polymers. Using a preshearing protocol that ensures a reproducible initial state ("rejuvenation" of the system), we report here the evolution of the flow curve from monotonically increasing to one dominated by a stress plateau, demonstrating a corresponding shear-banded state. Phenomenological understanding is provided through a scalar model that describes the free-energy landscape.

Soft materials are known to exhibit multiple dynamical processes ranging over logarithmic time scales from picosecond molecular segmental motion to reorganizations that are slow on a human time scale. Slow relaxations exhibited by many soft materials far from equilibrium are strongly reminiscent of the glassy dynamics observed in hard condensed matter, and their gradual slowing over time is referred to as "aging." Once aged, the resultant "soft glass" will typically exhibit a yield stress, below which it is predominantly elastic in its mechanical response and above which it freely flows. Under steady applied shear, such a material may subdivide, in a shear-banded manner, into fluidic and glassy states, separated by the yield stress and at which boundary aging and rejuvenation processes compete. The process of aging under shear may involve particle caging, but much slower mechanisms are often in evidence, suggesting the role of long-range cooperative effects. This leads to a "two-step" aging process, an idea we investigate here [1].

This continuous evolution of the mechanical and dynamical properties towards steady state has been the focus of much research. In particular, advancements have been made in the understanding of aging effects with the trap model introduced by Bouchaud [2] and later developed by Sollich *et al.* into the soft glassy rheology theory [3,4]. In these theories, mesoscopic "elements" traverse a free-energy landscape consisting of traps of various depths. Hopping between the traps is modeled by an effective activation temperature, the physical interpretation of which remains unclear, but which is intended to model in a mean field way, nonlinear couplings between the elements. An applied shear flow provides an external driving that hastens these local yielding events. A recent experimental investigation on a suspension of anisotropic and charged colloidal particles suspended in water [5] suggests colloidal gels and glasses are merely global minima in the same free-energy landscape. The typical aging experiment consists of putting the experimental system in a reproducible initial state (one that gives reproducible results), through either thermal or mechanical means, and allowing the system to evolve spontaneously for a time t_w, referred to as the "aging time" before performing the rheological test as a function of $t' = t - t_w$ where t' is the experimental time. Aging is usually manifested through a stiffening with increasing t_w, in shear start-up experiments and through a slowing down of relaxation rates. It is often possible to temporally rescale a series of aging experiments so as to yield universal curves [6,7].

Shear banding is not peculiar to glassy materials, but has been observed in wormlike micelles [8], emulsions near their yield stress [9], entangled polymer solutions [10], and liquid crystalline polymers [11], as well as recently in a nearly random close packed, hard-sphere colloidal suspension [12]. Shear banding has also been reported in dense pastes of large (0.29 mm) polystyrene beads [13]. Shear banding, identified experimentally through the coexistence of two or more bands of different viscosity or microstructure, is typically accounted for theoretically by a constitutive flow curve with an unstable branch of negative slope. When shear-rate conditions that correspond to the region of unstable flow are imposed, these systems can separate into phases of different local shear rates that coexist at a common stress. A recent review by Moller *et al.* [14] suggests shear banding, and thixotropy can be viewed as two effects of the same underlying cause. The fascinating question as to whether nonmonotonic constitutive behavior might be inherent to glassy yield-stress systems remains open.

Recent studies on high functionality star polymer [15] solutions have suggested both glassy dynamics and anomalous shear behavior [16]. In this Letter we examine the relationship between aging and shear banding. We note that star pair interactions depend strongly on their number of arms (functionality f) [17], and as f increases the tendency to hard-sphere behavior is increased. Helgeson *et al.* have shown suspensions of such stars form glasses [1] while reversible gelation due to thermal swelling has been found [18] in suspensions of these stars. Such properties suggest hitherto unknown behaviors that challenge conventional models of glassy behavior. Furthermore, the soft stars studied here provide one of the few examples of soft

matter in which the glass transition can be easily crossed via temperature and not volume fraction. In order to relate heterogeneous flow to the time dependent stress or strain rate constitutive properties, an experimental technique should combine rheomechanics with noninvasive velocimetry. In our approach time-resolved nuclear magnetic resonance (NMR) microscopy is the velocimetry of choice.

The main contribution of the present work is to perform the first experimental study of the interplay of aging and shear banding in a soft material where a distinct 2-step evolution is seen. We report rheological and rheo-NMR measurements on a system of star polymers with nominal functionality f, of 128 arms, each having nominal molecular mass, M_a, of 80 000 g/mol at a temperature of 293 K and at a concentration of $c = 2c^*$. Such stars exhibit behaviors intermediately between linear polymers and hard spheres, with evidence of both caging effects and soft interactions of the type associated with polymer entanglement. The current system therefore assists in elucidating how soft interactions that are not present in many hard-sphere systems manifest themselves on a macroscopic scale. An earlier rheo-NMR study by Holmes *et al.* [16] indicated intermittent shear-rate heterogeneity. However, that work, while on the same star polymer, was for a different solvent and at lower concentration, closer to c^*. It utilized a wide gap Couette cell with correspondingly wide stress variation across the gap, and used preshear protocols that differed in the case of the NMR and rheomechanical data. We here report on dynamics, involving both aging effects and shear banding, in the $c = 2c^*$ star polymer in squalene, for which consistent protocols are used and in which the rheo-NMR experiments are performed in a much narrower gap cell. We show the flow curve develops a stress plateau at low shear rates over the course of thousands of seconds, and that this in turn is associated with an evolution to a shear-banded state. We also show that a semiquantitative understanding can be gained from a simple scalar model.

In each experiment, a mechanical preshear protocol was followed, comprising a large amplitude oscillatory shear ($\gamma_0 = 100\%$, $\omega = 1$ rad s^{-1}) applied for a time 200 s. This placed the system in a reproducible history independent state. Figure 1 shows the stress response to a stepwise application of a shear rate for three different rates, $\dot{\gamma} = 0.001$ s^{-1}, 0.0025 s^{-1}, and 0.05 s^{-1}, performed on a strain-controlled ARES-HR rheometer equipped with a cone-and-plate geometry of diameter 25 mm, angle 0.04 rad, and truncation 48 μm. For $\dot{\gamma} = 0.001$ s^{-1}, the stress initially rises linearly with time or strain before reaching a metastable state where the stress $\sigma(\dot{\gamma})$, is a function of the applied shear rate after $\sim$100 s. For $\dot{\gamma} = 0.0025$ s^{-1}, the stress overshoots to a plastic limit before relaxing back to the metastable state. The system remains in this metastable state for $\sim$2000 s before the stress begins to increase towards the equilibrium value of
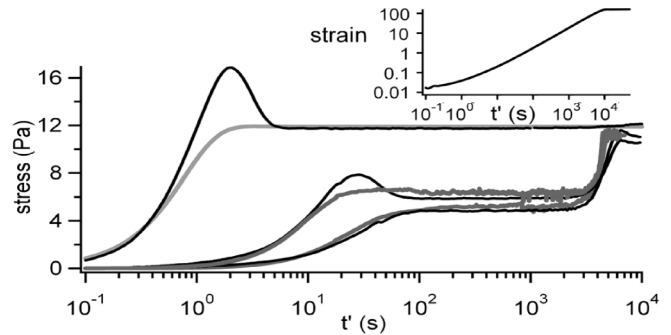

FIG. 1. Solid black lines: Experimental stress evolution upon shear start-up immediately following preshear, measured in the cone-and-plate geometry for the star polymer system and for shear rates $\dot{\gamma} = 0.001$ s^{-1} (lower line), $\dot{\gamma} = 0.0025$ s^{-1} (middle line), and $\dot{\gamma} = 0.05$ s^{-1} (upper line). Grey lines: Behavior of the phenomenological model. (Inset) Creep at 10 Pa, a stress less than the (evolved) yield stress showing flowing behavior up to $\sim 10^4$ s, after which the system solidifies.

$\sim$11 Pa. The duration of the metastable state increases with increasing shear rate up to a critical rate of $\dot{\gamma}_c = 0.035$ s^{-1}. It is thought that the time spent in the metastable state, clearly a function of the shear rate, is dictated by caging and entanglement effects. Above $\dot{\gamma}_c$, the metastable state is indistinguishable from the stable equilibrium state. Note the inset of Fig. 1, which shows that the system flows under an applied stress below the (evolved) yield stress, eventually aging to a solid at around 10^4 s.

Figure 2 shows the flow curve, measured in a downward rate sweep started at a time $t_w = 0$ after the preshear. At a shear-rate sweep residence time of 10 s per point (open circles), the flow curve indicates a shear thinning fluid.
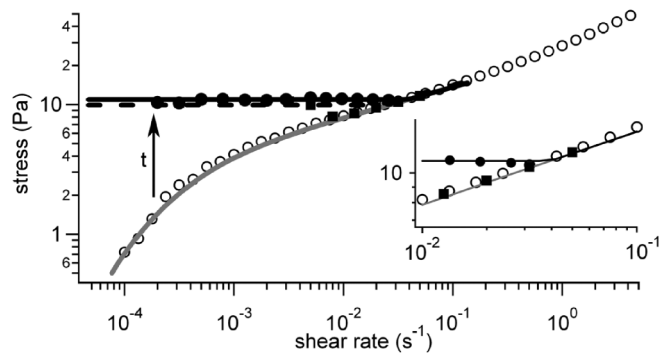

FIG. 2. Unfilled circles: Flow curve measured in cone-and-plate geometry on the star polymer system with a residence time of 10 s per point. Filled circles: Flow curve where the residence time is on the order of 10 000 s. Squares: Flow curve with residence time of 5000 s shown just in the vicinity of the crossover region. Solid lines: Behavior of the phenomenological model under identical conditions, grey = 10 s residence time, black = 30 000 s residence time. Dashed line: Model behavior for residence time of 5000 s. The inset shows an expanded view near the critical strain rate.

Figure 1 indicates that a residence time of 10 s samples the stress before reaching the metastable state at low shear rates. Having also seen from Fig. 1 that the stress takes on the order of 10 000 s to reach the stable state, we show a second rate sweep where the residence time is also of the order of 10 000 s (filled circles). What is apparent is a stress plateau that develops after thousands of seconds, with the plateau taking longer to reach as $\dot{\gamma}$ approaches $\dot{\gamma}_c$ from below. At intermediate times when the plateau is not fully formed, the flow curve exhibits a local minimum that can appear as a viscosity bifurcation in stress-controlled tests, as indicated by the black squares. When sufficient time has elapsed that the plateau is fully formed, no such bifurcation exists. Rates lower than 10^{-4} s^{-1} are difficult to access with the controlled strain rheometer, but creep experiments suggest a lower branch exists around 10^{-5} s^{-1}–10^{-6} s^{-1}, visible by slow accumulation of strain at long times for stresses $\sigma < \sigma_c$. This evolutionary behavior is contrasted with the case of wormlike micelles where any stress plateaux form rapidly.

Stress plateaux in flow curves have been linked to the phenomenon of shear banding. Figure 3 shows two velocity profiles across the 1.5 mm gap of a cylindrical Couette rheo-NMR cell at an apparent shear rate of 0.0314 s^{-1}, just below the critical strain rate, that were obtained at different times following the preshear protocol. The cell has inner and outer radii of 7.5 mm and 9 mm. The unfilled circles show the velocity profile across the cell at time $t' = 150$ s, which corresponds to the open circles of Fig. 2. The filled circles show the velocity profile at $t' = 25\,000$ s and reveal a banded structure where the lower shear-rate band has a shear rate ~ 0 s^{-1}. The small value of the shear rate indicates an increase in the viscosity, similar to that observed by Coussot *et al.* [19]. However, the data of Fig. 1, in particular, the lack of thixotropy, the stress overshoot,
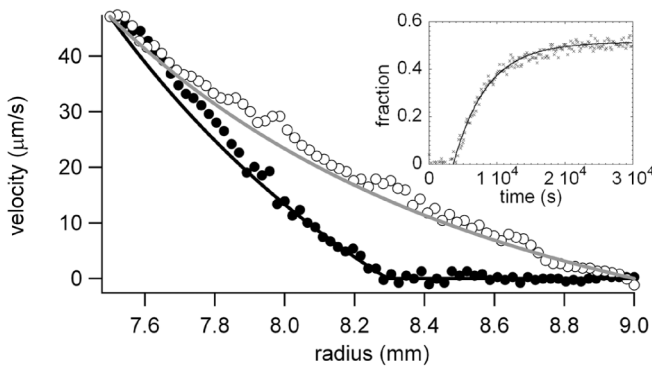

FIG. 3. Black unfilled circles: Velocity profile across the 1.5 mm gap of the cylindrical Couette at an apparent shear rate of 0.0314 s^{-1} at time $t' = 150$ s following preshear. Black filled circles: Velocity profile under the same conditions at a time $t' = 25\,000$ s. Solid lines: Behavior of the phenomenological model under identical conditions. Grey: $t' = 150$ s. Black: $t' = 25\,000$ s. Inset: The evolution of the jammed fraction (points) fitted by an exponential growth (solid line).

and the long time before stiffening, suggests that different physics is responsible. The central cylinder is filled with a marker fluid so the inner wall velocity is known. No slip is seen during the evolution. The low shear-rate band evolves across the gap from the outer wall to reach a final fraction dictated by the applied shear rate, as shown in the inset of Fig. 3. The growth of the low shear-rate band can be modeled by an asymptotic exponential growth.

Motivated by the two-state evolution apparent in Figs. 1–3, we suggest the following physical picture. The large stresses that arise during the oscillatory preshear ensure a fluidized state at the start of each experiment. In this state, the system flows homogeneously with a flow curve shown by the open symbols in Fig. 2. At stresses below the critical yield value σ_c, however, this fluidized state is metastable. Under conditions of imposed shear rate $\dot{\gamma} < \dot{\gamma}_c$, this results in the formation of a solidified band that coexists with a fluid band at the critical stress σ_c. At stresses above σ_c, in contrast, the system remains fluidized. In summary, the system undergoes stress dependent switching between solidified and fluidized states, which can coexist under conditions of imposed shear rate.

We now present a rudimentary model aimed at capturing this phenomenology. In the spirit of the fluidity models of Picard and Ajdari [20] we assume that the stress $\sigma = \sigma(t)$ evolves according to

$$\partial_t \sigma = G\dot{\gamma} - a^2 \sigma. \qquad (1)$$

Here the first term on the right-hand side corresponds to the elastic development of stress under an applied shear. To allow for shear-banded states, the shear rate $\dot{\gamma} = \dot{\gamma}(y, t)$ can depend on the distance y across the rheometer gap. The modulus G is assumed constant. The second term confers stress relaxation on a time scale $1/a^2$. The dynamics of the corresponding fluidity a^2 obeys

$$\partial_t a(y, t) = -M \frac{\delta V(\sigma, a)}{\delta a} + l^2 \partial_y^2 a + N(y, t). \qquad (2)$$

Suppressing for the moment any spatial dependence upon y such that $a = a(t)$, $N = N(t)$ only, at a fixed stress σ the first term on the right-hand side describes descent in an effective potential V at a rate set by the mobility M. Alone, this term would ensure that the system descends until its first encounter with a local minimum of V, in which it remains thereafter. The delta correlated noise N models thermal and mechanical agitation, and confers a stochastic way of exploring the potential landscape such that the system can eventually find the global minimum.

We show in Fig. 4 the form of V chosen to match the two-state phenomenology seen in the experiments. To incorporate both fluidized and solidified states, we take

$$V = \frac{a^6}{3} - \frac{[\alpha(\sigma) + \beta(\sigma)]a^4}{2} + \alpha(\sigma)\beta(\sigma)a^2 \qquad (3)$$

with $0 < \alpha < \beta$. By construction, this has a minimum
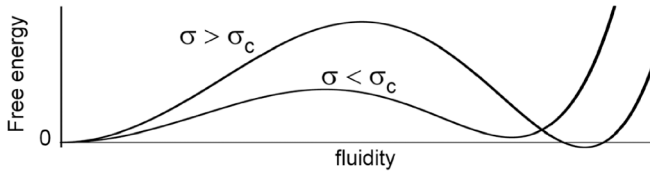
FIG. 4.   The shape of the free-energy-type function for stresses
below and above the critical stress.

representing a high fluidity state at $a^2 = \beta$, and a mini-
mum representing a solidified state at $a = 0$. It can be
shown that for β less (greater) than 3α the solidified
(fluidized) state is the global minimum. Stress dependent
switching between these two states is captured by letting
$\alpha = \alpha(\sigma)$ and $\beta = \beta(\sigma)$, with β a more steeply increas-
ing function of σ such that switching occurs at the critical
value of the stress $\sigma = \sigma_c$ for which $\beta = 3\alpha$. For conve-
nience, we choose the following functional forms:

$$\alpha = A + B\sigma^n, \quad \text{and} \quad \beta = B + B\sigma^m, \qquad (4)$$

with $m > n$. From Eqs. (3) and (4) it can be shown that σ_c
is the stress at which $\alpha = \beta/3$ and in our parametrization
takes the value 11.2 Pa. While the basic phenomenology of
the model is quite robust with respect to different values of
the parameters A, B, n, m, l, here we make specific choices
$A = 4.2 \times 10^{-3}$, $B = 8.3 \times 10^{-3}$, $n = 2.845$, $m = 3.3$,
$l = 0.01$. These were obtained by first adjusting the pa-
rameters A, B, n, and m to represent the two flow curves of
Fig. 2, obtained, respectively, at the limits of short and long
time, and l along with the noise term N, to represent the
time dependence of $\sigma(t)$ (Fig. 1). This noise is represented
by a random value from a Gaussian distribution such that
the standard deviation equals $\frac{1}{6}(\alpha - \beta)^3$, the height of the
barrier between the two nonzero fluidity minima.

    The predictive power of the model can be tested by using
the above parameter set to generate the velocity profiles of
Fig. 3. The description of shear banding at an imposed
shear rate $\bar{\gamma} = \int dy \dot{\gamma}(y, t)$ requires the term $l^2 \partial_y^2 a$ to cor-
rectly represent the structure of the interface between the
bands, with a characteristic width l, expressed as a fraction
of the gap traversed by y. As shown in Figs. 1 and 2, the
model captures the basic phenomenology and, further,
predicts good agreement with the velocimetry data shown
in Fig. 3. In a shear start-up experiment, and following the
preshear protocol (Figs. 1 and 2), the stress attains the
fluidized branch of the flow curve, on which the system
flows homogeneously. For values of the shear rate $\bar{\gamma} < \dot{\gamma}_c$,
the stress subsequently evolves towards its final value σ_c,

at which a solidified band coexists with a fluid band.
Likewise in a shear-rate sweep (Fig. 2), the model predicts
the fluidized homogeneous flow branch shown by the gray
line for fast sweep rates, and a yield stress at which fluid-
ized and solidified bands coexist for slow sweep rates.

    The model system examined here manifests a two-step
aging property that may underpin a wide class of yield-
stress fluids. That we can, by using such a simple phe-
nomenological model, capture the time dependence of both
the stress and shear-rate profile on steady shear start-up, as
well as the time-dependent flow curve, suggests the possi-
bility of a universal description for aging rejuvenation and
shear banding dynamics in soft glasses.

    *Author to whom correspondence should be addressed.
    paul.callaghan@vuw.ac.nz
 [1] M. E. Helgeson *et al.*, J. Rheol. (N.Y.) **51**, 297 (2007).
 [2] J. P. Bouchaud, J. Phys. I (France) **2**, 1705 (1992).
 [3] P. Sollich *et al.*, Phys. Rev. Lett. **78**, 2020 (1997); Phys.
     Rev. E **58**, 738 (1998).
 [4] S. Fielding *et al.*, J. Rheol. (N.Y.) **44**, 323 (2000).
 [5] S. Jabbari-Farouji *et al.*, Phys. Rev. Lett. **99**, 065701
     (2007).
 [6] C. Derec *et al.*, Phys. Rev. E **67**, 061403 (2003).
 [7] M. Cloitre *et al.*, Phys. Rev. Lett. **85**, 4819 (2000).
 [8] M. M. Britton *et al.*, Phys. Rev. Lett. **78**, 4930 (1997).
 [9] P. Coussot *et al.*, Phys. Rev. Lett. **88**, 218301 (2002).
[10] P. Tapadia and S.-Q. Wang, Phys. Rev. Lett. **91**, 198301
     (2003).
[11] C. Pujolle-Robic and L. Noirez, Nature (London) **409**, 167
     (2001).
[12] L. Isa *et al.*, Phys. Rev. Lett. **98**, 198305 (2007).
[13] N. Huang *et al.*, Phys. Rev. Lett. **94**, 028301 (2005).
[14] P. C. F. Moller *et al.*, Soft Matter **2**, 274 (2006).
[15] J. Roovers *et al.*, Macromolecules **26**, 4324 (1993).
[16] W. M. Holmes *et al.*, J. Rheol. (N.Y.) **48**, 1085 (2004).
[17] C. N. Likos *et al.*, Phys. Rev. Lett. **80**, 4450 (1998).
[18] M. Kapnistos *et al.*, Phys. Rev. Lett. **85**, 4072 (2000).
[19] P. Coussot *et al.*, Phys. Rev. Lett. **88**, 218301 (2002).
[20] G. Picard *et al.*, Phys. Rev. E **66**, 051501 (2002).